Battery Power Requirements in High-Performance Electric Vehicles

Quirin Kellner, W. Dhammika Widanage, James Marco
WMG, University of Warwick
q.kellner@warwick.ac.uk

***Abstract*- International standards and guidelines regarding characterisation and cycle life testing of batteries in electric vehicles (EVs) currently do not take into account high-performance driving. Using simulation software, track driving in a high-performance vehicle is simulated, and speed-time profiles are recorded. These as well as established driving cycles are used in conjunction with an EV model to determine power profiles at battery terminals. The difference in the resulting power profiles suggest that the evaluation of batteries for the HP segment requires separate characterisation and cycle life tests.**

I. INTRODUCTION

The automotive sector is currently experiencing a surge in electro mobility with electric vehicles (EVs) gaining increased market share [1]. However, limited range and battery life, slow recharge time and high initial cost of the batteries are still major stepping stones for EV acceptance in the mass market [2]. In order to determine a battery's suitability for automotive use manufacturers of battery electric vehicles (BEVs) and researchers use testing procedures that represent the conditions the battery encounters during its life. The representability of these procedures is of paramount importance as operating conditions play a major role in the behaviour and degradation of a battery [3].

International (draft) standards and guidelines such as ISO-12405 [4] , IEC-62660 [5], and the United States Advanced Battery Consortium (USABC) Battery Test Manual For Electric Vehicles [6] were developed for battery and cell testing and characterisation to cover a range of scenarios during a cell's useful life in EVs. These testing scenarios include standard tests for charge and discharge, performance, reliability, abusive, and cycle life tests. The aim of the cycle life tests is the simulation and evaluation of battery life in EVs. In order to ensure that cycle life tests are representative of everyday operation of the battery the cycle life tests in these standards are losely based on driving cycles. The "Dynamic Stress Test" as described in [6] for example is a simplified version of the power profile that is produced when the Federal Testing Procedure (FTP-75) driving cycle is applied to a specific EV [7]. Some other studies investigating cycle life testing of batteries use different established driving cycles in combination with simple vehicle models [8], [9] or their own real life driving data [10], [11] to develop cycle life testing cycles.

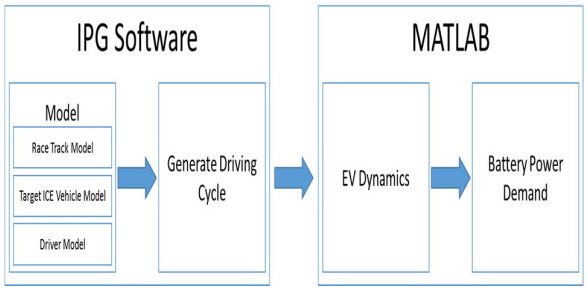

Fig. 1. Methodology for HPEV battery duty cycle generation

One vehicle segment attracting increasing interest is the "high-performance" (HP) segment [12] with vehicles such as the Tesla Model S, the Rimac Concept_One and Concept_S. During their everyday operations on public roads these vehicles are usually restricted by traffic and/or speed regulations. Opportunities to fully utilise such a vehicle are limited to driving on designated racing tracks, where traffic and speed limits do not usually apply and the performance is likely to be limited by the vehicle and/or driver. As such track or HP driving is different to driving on the open road, and for BEVs a different power demand for the battery is expected. It is therefore necessary to understand the differences in power demand between HP and "everyday" driving to determine whether the existing testing procedures could adequately capture HP power demand.

Real life testing on tracks with a HP vehicle is expensive and requires a large amount of resources. This can be overcome by using capable software to simulate a representative speed-time profile, which can then be converted to a power profile for a battery pack. This paper presents a novel approach to determine battery power profiles during track driving in an HP vehicle, and quantifies differences in battery power demand between track and everyday driving.

II. METHODOLOGY

The proposed methodology is summarised in Fig. 1. Nine racing tracks (Table 1) were modelled in IPGRoad and a conventionally powered target vehicle was modelled in IPGCarMaker (Table 2) and validated against published data. Driving was simulated with IPGDriver's integrated race driver. The mentioned software packages are tools used in industry and have been validated in several use cases [13]–[15]. These models were used to generate speed-time profiles or driving cycles for HP driving.

Subsequently an EV dynamics model in MATLAB was used to determine the battery power demand at the pack terminals for these HP driving cycles and 11 established driving cycles (Table 3).

978-1-5090-0403-4/16/$31.00 ©2016 IEEE

TABLE I
RACE TRACK MODEL OVERVIEW

Track	Model Length (km)	Official Length (km)	Delta (%)	Number of corners
Dunsfold Park (Top Gear)	2.852	2.818	1.22	8
Anglesey International Circuit	3.294	3.381	-2.57	10
Goodwood Full Circuit	3.853	3.832	0.55	9
Brands Hatch Grand Prix Circuit	3.908	3.917	-0.23	10
Lausitzring Automobilsport	4.551	4.534	0.37	14
Nurburgring GP	5.142	5.148	-0.12	16
Suzuka GP	5.828	5.807	0.36	18
Silverstone GP	5.920	5.892	0.46	17
Nurburgring Nordschleife	20.800	20.832	-0.15	73

A. IPG Software Modelling

The track lengths range from 2.8 to 20.8 km, and from 8 to 73 corners. The track models deviate from official circuit length by 6m to 87m. This deviation translates to an error of 2.5% in the worst case but lower than 1% in most cases, which was assessed to be acceptable. Road elevation and inclination was ignored for simplification. Ignoring road inclination and the resulting gravitational forces on the vehicle influences the speed profile of a vehicle driving on a track. It is expected that a driver will push the vehicle to its performance limits. With reference to power demand driving uphill then would result in a longer demand in power for propulsion and a shorter braking duration. Similarly, for driving downhill, the duration of peak power demand will be shorter, whereas the braking duration increases. This simplification is equivalent to a vehicle driving on a track with longer/shorter straights. However due to the variety of tracks chosen the overall characteristics of HP driving are expected to not be influenced. Additionally due to time constraints of the work, and no access to surveying data from the tracks, the additional modelling required to fully represent the racing tracks has been ignored.

The target vehicle for this research is what is referred to in popular media as a “Supercar”. CarMaker supplies a range of example demonstration vehicle models including a high performance vehicle similar to an Audi R8 Coupe with a 4.2l V8 engine and 4 wheel drive. This model was adapted to match acceleration times from 0-100 km/h, 0-200km/h, and top speed compared to data published by Audi [16], and ‘Car & Driver’ (C&D) [17]. For acceleration times the model performed within an error of 10%. Due to the fidelity of the source data and model it was concluded that a better accuracy would be impractical.

Subsequently IPG-Driver was used. The software offers an artificial intelligence (AI) driver which is a controller for following a course and a speed on a given track. The integrated driver model adaption was run for a virtual race driver to learn the limitations of the vehicle. Information about the functionality of IPG-Driver can be found in [18].

These three models were then used simulate driving of a vehicle in track scenarios to generate speed-time profiles or driving cycles.

TABLE II
HIGH PERFORMANCE VEHICLE MODEL PARAMETERS

Parameter	Value
Vehicle body	Rigid body
Vehicle mass	1560 (kg)
Wheelbase	2.60 (m)
Height of centre of gravity	0.5 (m)
Longitudinal drag coefficient	0.3
0 – 100 km/h	4.1 (s)
0 – 200 km/h	13.9 (s)
Top Speed	301 (km/h)

B. EV Model

These resulting profiles were used in combination with a wheel-to-battery EV model based on the architecture in Fig. 2 to calculate the power profile at battery pack terminals for an EV competing with the conventionally powered vehicle.

Many vehicles in the HP segment use rear-wheel drive (RWD) or all-wheel drive (AWD). By using a RWD architecture a large portion of the braking force is lost to heat. The utilisation of separate front and rear electric machines allows for a larger proportion of the braking force to be used for regenerative braking. Similarly to the model used in the benchmarking CarMaker simulations the EV is assumed to have a AWD system, which allows for faster accelerations. The power for propulsion however does not originate from an internal combustion engine but from two electric machines. One for the front wheels and one for the rear wheels.Using a model as found in literature in combination of a power split ratio for front and rear wheels of 30-70 during traction and 70-30 during braking, respectively, it is possible to determine the power demand at the wheels [19]. For simplification only the longitudinal components of acting forces are regarded. The longitudinal dynamics of the vehicle model are described in (1) – (2).

TABLE III
ESTABLISHED DRIVING CYCLES

Driving Cycle	Duration (s)	Distance (km)
NEDC	1184	10.9
Artemis Urban	993	4.9
Artemis Rural	1082	17.3
Artemis Motorway	1068	29.6
FTP-75	2477	17.7
HWFET	765	16.5
EPA-US06	600	12.9
EPA-SC03	594	5.8
Japan 10-15 Mode	891	6.3
Japan JC08	1215	8.2
LA92	1435	15.8
WLTP Class 3	1800	23.3

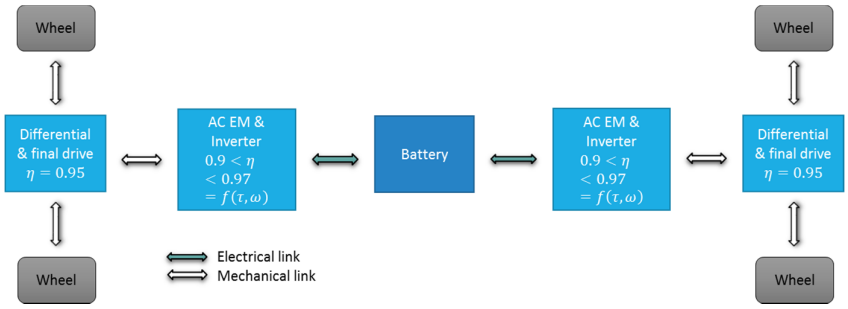

Fig. 2. HP EV powertrain architecture

$$F_{Tr} = m_v \frac{dv}{dt} + \frac{1}{2}\rho_A C_D A_f v^2 + m_v g k_{RR} \quad (1)$$

$$F_{Tr} = Tr_{Front} + Tr_{Rear} \quad (2)$$

m_v is the vehicle mass, Tr_{Front} and Tr_{Rear} are the traction forces at front and rear axle, F_{RR} is the rolling resistance, ρ_A is the density of air, C_D is the drag coefficient, A_f is the effective 2-D vehicle frontal area, v is the vehicle velocity, g is the standard acceleration due to gravity, and k_{RR} is the coefficient of rolling resistance.

Ground adhesion between tyre and road is a limiting factor, hence it is necessary to include tyre dynamics. The tractive effort in relation to a torque applied to a wheel with dynamic rolling radius r_{wdyn} is expressed in (3) and illustrated in Fig. 3. The maximum tractive effort that the tyre and road can support is given in (4), and depends on the reaction force of the ground on the wheel (W_{Wheel}) and the dynamic coefficient of tyre adhesion (μ), which is a function of wheel slip (λ) as in (5) – (6).

$$F_{Tr} = \frac{T}{r_{wdyn}} \quad (3)$$

$$F_{TrWheel_{Max}} = W_{Wheel} * \mu \quad (4)$$

$$\mu = f(\lambda) \quad (5)$$

$$\lambda = \frac{\omega r_{wdyn} - v}{\max(v, \omega r_{wdyn})} \quad (6)$$

Wheel slip data recorded during CarMaker simulations and is used for the EV model. Wheel slip for front and rear wheels is different due to the different reaction forces during acceleration and braking. Hence front and rear rotational speeds are expressed separately (7) – (10).

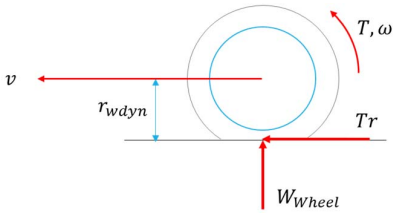

Fig. 3. Forces acting on a tyre

$$Tr_{Front} = \begin{matrix} 0.3 * F_{Tr} & \text{for } F_{Tr} > 0 \\ 0.7 * F_{Tr} & \text{for } F_{Tr} < 0 \end{matrix} \quad (7)$$

$$T_{Front} = Tr_{Front} * r_{wdyn} \quad (8)$$

$$\omega_{Front} = \frac{(1-\lambda)v}{r_{wdyn}} \quad (9)$$

$$P_{Front} = T_{Front} * \omega_{Front} \quad (10)$$

As the maximum rotational speed of the wheels may not be synonymous with the maximum rotational speed of the electric machine of choice, a gearing ratio, $\zeta_{Diff} = 3$, is assumed to be incorporated in the differential as a final drive and the efficiency (η_{Diff}) is assumed to be 95%. Efficiency maps for the motor-inverter assembly (η_{IF}) are based on real testing data provided by an industrial partner and scaled to suit the power demand at front and rear wheels at maximum vehicle speed. This would allow for an excess power potential at lower vehicle speeds. Alternatively matching the top vehicle speed to the rotational speed where the motor shows its maximum power would eliminate the top range of the operational speeds of the motor. As a third option the implementation of a multispeed gearbox would allow for further optimisation of the EM sizing. For this study the first mentioned approach was chosen as to avoid over-engineering of the power train system, and keeping powertrain weight to a minimum.

The operating points for a high performance scenario are shown in Fig. 4. During traction (power > 0) they lie within the operating capability of the electric machines. The power available for regenerative braking (power < 0) is restricted by the capability of the electric machines. For the rear electric machine all power available for regenerative braking could be harvested. At the front, the power has to be restricted to the machine's maximum capability based on rotational speed. The power demand at pack terminals is inverted such that charging power is +ve and discharging power is –ve. Power at the battery pack terminals (P_{Batt}) is calculated as in (11)-(12).

$$P_{IF} = \begin{matrix} \frac{P_{Front}}{\eta_{Diff} * \eta_{IF}} & \text{for } P_{Front} > 0 \\ P_{Front} * \eta_{Diff} * \eta_{IF} & \text{for } P_{Front} < 0 \end{matrix} \quad (11)$$

$$P_{Batt} = -(P_{IF} + P_{IR}) \quad (12)$$

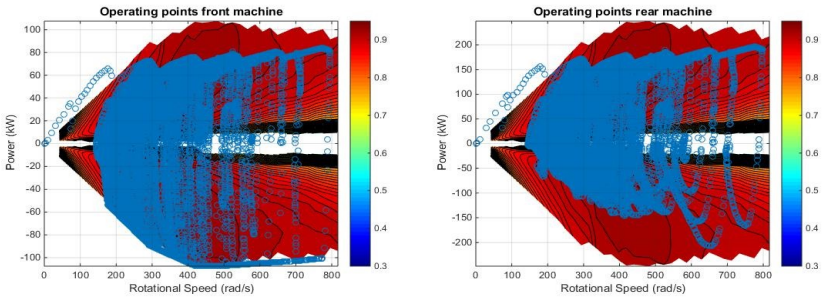

Fig. 4. Efficiency maps and operating points for the front and rear electric machines

P_{IF} and P_{IR} is the power at the front and rear inverters, respectively. The calculation for power at the rear motor is synonomys with (11).

III. RESULTS AND DISCUSSION

Fig. 5a & 5b show the mean (a) and peak (b) discharging (green, -ve) and charging (red, +ve) power demand on the battery pack for normal and HP cycles. It can be clearly seen that the power demand for HP cycles is much larger than the demand for normal driving. This can be attributed to higher rate accelerations and higher peak and mean speeds. A battery pack designed for road use therefore would be pushed to if not beyond its power and current limits. With higher charging and discharging currents, ohmic heat losses increase exponentially at I^2 R, and the temperature of the cells increases, accelerating ageing.

As the normal cycles do not take into account aggressive driving on the road, it is difficult to determine a definite threshold for HP in terms of mean and peak power demand for charging and discharging. However based on the graphs a first approximation as a threshold for "above normal" demand can be made for the existing vehicles. These are in graph a) -50 kW for mean discharging power and 25 kW for mean charging power. Similarly for peak power values, a first approximation can be made for "above normal" demand at 100kW charging and -125kW discharging power.

Fig. 5c shows the variable Φ_{Cycle} (defined in (13)) for charging (red) and discharging (green) power demand.

$$\Phi_{Cycle} = \frac{mean\ power\ demand}{\max power\ demand} \tag{13}$$

It is a measure between of how close the mean power demand is to the peak power requirements for each driving scenario. A value close to 1 indicates that the continuous power demand on the battery pack is similar to the peak power demands of the battery pack. As such, a battery operating close to its maximum power and current capability will also show an increase in thermal losses and operating temperature. A value close to zero indicates that the continuous power demand of the battery is a small fraction of the peak power demand. This should be taken into account during battery pack specification. A pack designed for a low mean power demand with short peak bursts can be significantly smaller than a pack designed for high continuous power demand, as cooling is less important. This raises the question whether or not there is a potential need for hybrid packs, where peak power bursts are covered by supercapacitors. Additionally a pack designed for lower power demand could contain fewer cells as each cell has to endure lower mean currents. Subsequently battery weight and size could be reduced.

The graph shows that HP cycles tend to show larger values of $\Phi_{Cycle} \geq 0.5$ for discharge than the normal cycles (≤ 0.45), with smaller values for city cycles and larger values for motorway cycles. The difference for charge however is not apparent as the Japanese 10-15 mode displays the highest ratio. This is down to the fact that the mean charging power is permanently close to the peak, although the absolute charging power demand is more than a magnitude smaller than it is for HP cycles.

The latter can be observed in Fig. 5d. The variable Φ_{System} as defined in (14) shows how the mean power demand compares to the system peak power. The system power is the peak power that the electric machines can provide, which is 355kW.

$$\Phi_{System} = \frac{mean\ power\ demand}{system\ power} \tag{14}$$

Here the HP cycles outperform the normal cycles by a factor of 4.8 based on the highest value for normal cycles (Artemis Motorway) and lowest value for HP cycles (Lausitzring). This indicates that a pack designed for HP power demand would require significantly more thermal control, or higher capacity than a pack designed for normal road use. For this particular vehicle an approximation can be made again to distinguish normal performance from "above normal" performance. In this case if $\Phi_{System} > 0.1$, it can be concluded that the vehicle is performing at higher than normal demand. Although this value is valid only for this vehicle the process is valid for any case study.

The four measures illustrated in Fig. 5a-d are helpful in highlighting the differences between HP and normal cycles but the absolute values of these measures are heavily system related for the HP cycles. If the target vehicle was limited to a maximum power output of 95kW (just sufficient to complete the EPA-US06 cycle), the values for HP cycles would be smaller for mean and peak power demand, and larger for Φ_{Cycle} due to a longer duration in acceleration periods, and larger

values for normal cycles for Φ_{System} due to the reduction in system peak power. Similarly, a vehicle with much larger power capability would produce faster HP cycle velocities and accelerations and display larger values for mean and peak power.

Fig. 5e shows the mean power demand for the battery pack of the target vehicle for normal and HP driving. HP mean power demand ranges from 52.7 kW – 79.4 kW, and normal driving demand ranges from 1.9 kW – 21.5 kW discharging power, showing a stark contrast between HP and normal power demand.

Fig. 5f shows the net energy required per km. The least net energy intensive HP cycle (Silverstone) requires 2.3 times as much energy per km as the most demanding normal cycle (Artemis Motorway). Upon comparison with the current emission testing cycles for Europe (NEDC) and the U.S. (FTP75), this factor increases to 4.0 and 4.1, respectively. It is noteworthy that although the FTP75 procedure is more aggressive than the NEDC cycle, the regenerative braking capability on this particular target vehicle results in similar energy requirements per km. The "above normal" net energy demand per km is at -0.25 kWhkm^{-1}.

Papers have suggested that battery ageing progresses with total energy throughput [20], [21]. In Fig. 5g it can be seen that the total energy throughput per km for HP cycles is 3 times higher than it is for normal cycles. A pack designed for normal road use that is used for HP driving would therefore have reduced lifetime based on distance driven, regardless of temperature dependent degradation processes. The "above normal" approximation here lies at 0.5 kWhkm^{-1}.

Apart from absolute and relative values of power demand the frequency and duration of power pulses are equally as important to determine the characteristics of the HP cycles and differences to normal cycles. As such the power profiles were analysed using the measure κ_W which is percentage of time the battery is either charging or discharging (Fig. 5h). As HP cycles do not encounter any naturally occurring stops as is the case during urban driving, the battery is expected to be under

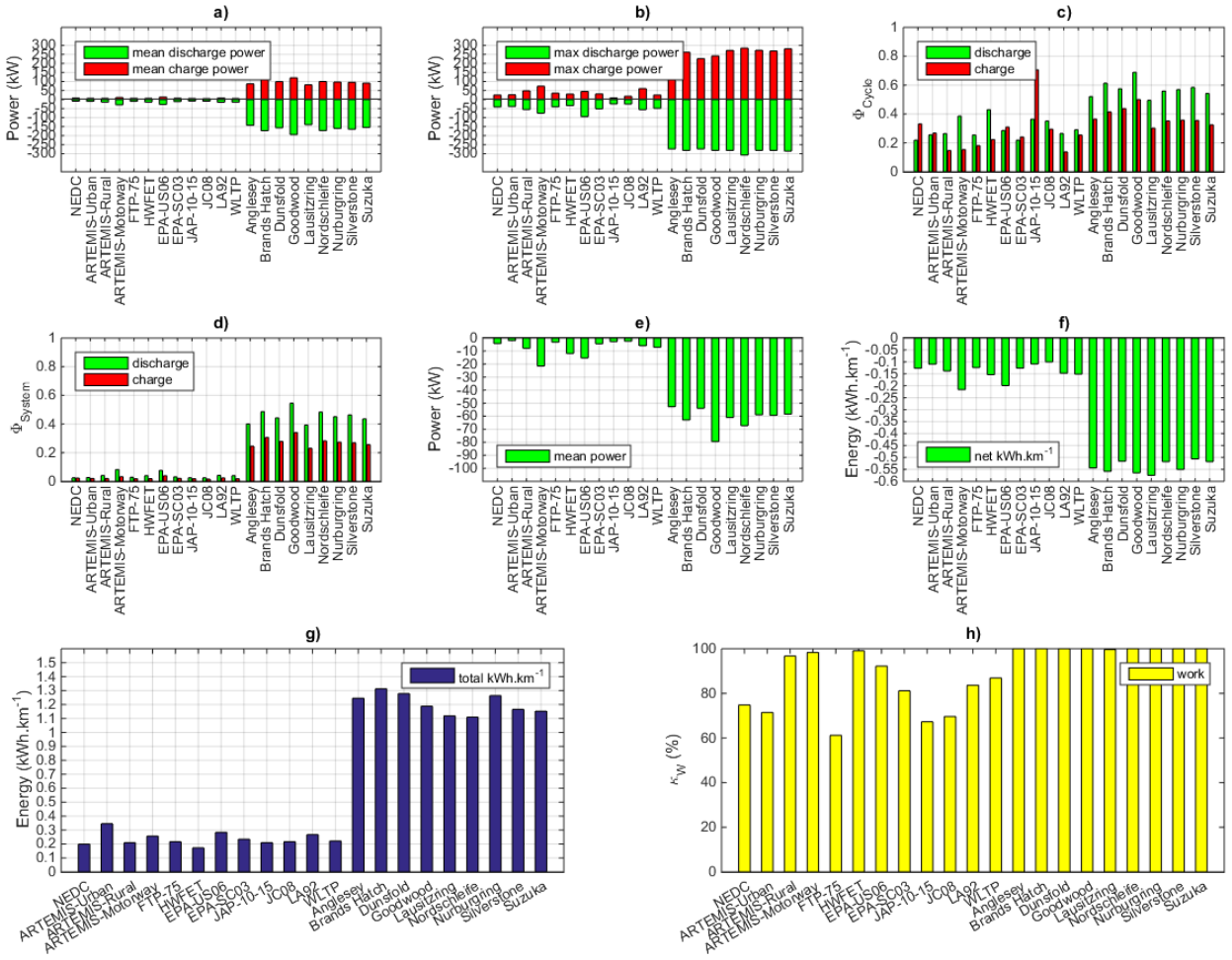

Fig. 5. a) mean charging and discharging power per cycle; b) maximum charging and discharging power per cycle; c) Cycle based power factor(Φ_{Cycle}); d) System based power factor (Φ_{System}); e) mean power during cycle; f) net energy demand per km; g) total energy throughput per km; h) % of time working (charge and discharge)

constant stress. A higher performing vehicle could spend a lower amount of time accelerating/ discharging the battery but would have deceleration times still limited by tyre dynamics hence would have a different split of charge to discharge, but still a similar value for κ_W.

IV. CONCLUSIONS AND FURTHER WORK

There is a large difference in battery pack power demand between the track driving scenarios and normal driving. This difference in power demand is also likely to have an effect on the ageing and thermal behaviour of the cells within the battery pack. If a pack is designed for everyday driving and is used in a track scenario then the pack may not deliver the power required or last only for a very short time. A pack specified for track use may be inadequately large, heavy or expensive for everyday use. As such it can be concluded that existing testing procedures are not sufficient and that it is necessary to use separate characterisation and cycle life testing profiles to evaluate batteries for the HP segment. Based on this work a battery duty cycle representative of HP driving will be developed for use in cycle life battery degradation studies.

V. ACKNOWLEDGMENTS

The research presented within this paper is supported by the Engineering and Physical Science Research Council (EPSRC-EP/M507593/1). The research was undertaken in collaboration with the WMG Centre High Value Manufacturing Catapult (funded by Innovate UK) in collaboration with Jaguar Land Rover and Delta Motorsport.

REFERENCES

[1] Y. Zhou, M. Wang, H. Hao, L. Johnson, H. Wang, and H. Hao, "Plug-in electric vehicle market penetration and incentives: a global review," *Mitig. Adapt. Strateg. Glob. Chang.*, 2014.

[2] C. C. Chan, "The state of the art of electric, hybrid, and fuel cell vehicles," *Proc. IEEE*, vol. 95, no. 4, pp. 704–718, 2007.

[3] A. Barré, F. Suard, M. Gérard, M. Montaru, and D. Riu, "Statistical analysis for understanding and predicting battery degradations in real-life electric vehicle use," *J. Power Sources*, vol. 245, pp. 846–856, Jan. 2014.

[4] ISO, "BS ISO 12405-2:2012 Electrically propelled road vehicles — Test specification for lithium-ion traction battery packs and systems." ISO, Geneva, 2012.

[5] International Electrotechnical Commission, "IEC 62660-1." Geneva, 2010.

[6] Idaho National Laboratory, "U . S . Department of Energy Vehicle Technologies Program Battery Test Manual For Plug-In Hybrid Electric Vehicles - Revision 3," *U.S. Department of Energy*, no. March. pp. 16–18, 2015.

[7] E. C. Castillo, *Standards for electric vehicle batteries and associated testing procedures*. Elsevier Ltd., 2015.

[8] S. B. Peterson, J. Apt, and J. F. Whitacre, "Lithium-ion battery cell degradation resulting from realistic vehicle and vehicle-to-grid utilization," *J. Power Sources*, vol. 195, no. 8, pp. 2385–2392, 2010.

[9] M. T. Lawder, P. W. C. Northrop, and V. R. Subramanian, "Model-Based SEI Layer Growth and Capacity Fade Analysis for EV and PHEV Batteries and Drive Cycles," *J. Electrochem. Soc.*, vol. 161, no. 14, pp. A2099–A2108, 2014.

[10] A. Devie, E. Vinot, S. Pelissier, and P. Venet, "Real-world battery duty profile of a neighbourhood electric vehicle," *Transp. Res. Part C Emerg. Technol.*, vol. 25, pp. 122–133, 2012.

[11] F. P. Tredeau and Z. M. Salameh, "Evaluation of Lithium iron phosphate batteries for electric vehicles application," *2009 IEEE Veh. Power Propuls. Conf.*, pp. 1266–1270, 2009.

[12] W. Sierzchula, S. Bakker, K. Maat, and B. Van Wee, "The competitive environment of electric vehicles: An analysis of prototype and production models," *Environ. Innov. Soc. Transitions*, vol. 2, pp. 49–65, 2012.

[13] S. a. Oleksowicz, K. J. Burnham, A. Southgate, C. McCoy, G. Waite, G. Hardwick, C. Harrington, and R. McMurran, "Regenerative braking strategies, vehicle safety and stability control systems: critical use-case proposals," *Veh. Syst. Dyn.*, vol. 51, no. May 2015, pp. 684–699, 2013.

[14] U. Wurster and I. P. G. A. Gmbh, "Substantial Progress of Virtual Driver Skills in Interaction with Advanced Control Systems to meet the new Challenges of Vehicle Dynamics Simulation," in *10th International Symposium on Advanced Vehicle Control*, pp. 852–860.

[15] IPG Automotive, "IPG CarMaker User's Guide (v4.5.5)." Karlsruhe, 2014.

[16] Audi United Kingdom, "R8 Coupé," 2015. [Online]. Available: http://www.audi.co.uk/new-cars/r8/r8-coupe.html#/R8 V8. [Accessed: 18-Jun-2015].

[17] Car and Driver, "R8 Coupe Manual Quattro V8," 2015. [Online]. Available: http://buyersguide.caranddriver.com/audi/r8/specs#features.

[18] IPG Automotive, "IPGDriver User Manual 6.4." pp. 1–153, 2014.

[19] M. Eshani, Y. Gao, S. Gay, and A. Emadi, *Modern electric, hybrid electric and fuel cell vehicles 2nd. Edition*. 2010.

[20] J. Groot, M. Swierczynski, A. I. Stan, and S. K. Kær, "On the complex ageing characteristics of high-power LiFePO4/graphite battery cells cycled with high charge and discharge currents," *J. Power Sources*, vol. 286, pp. 475–487, Jul. 2015.

[21] C. Guenther, B. Schott, W. Hennings, P. Waldowski, and M. a. Danzer, "Model-based investigation of electric vehicle battery aging by means of vehicle-to-grid scenario simulations," *J. Power Sources*, vol. 239, pp. 604–610, 2013.